GRIDLESS 2D RECOVERY OF LINES

KÉVIN POLISANO, BASILE D. BONAIRE, SYLVAIN MEIGNEN

PROBLEM

Recovery of altered lines in blurry and/or noisy situation

- Recovery of the number K of 2D lines,
- Recovery of their amplitude α_k and position $\boldsymbol{x_k}$,
- Adaptable to different kernels φ.

Algorithm used: **Sliding Frank-Wolfe**, by Denoyelle et al. [1].

GENERAL MODEL

Definitions

- $\mathcal{X} = \mathbb{R} \times \left(-\frac{\pi}{2}, -\frac{\pi}{2}\right]$ space of parameters
- $\mathcal{H} = \mathbb{R}^{N^2}$ Hilbert space of sampled realizations
- $\mathcal{M}(\mathcal{X})$ space of Radon measure over $\mathcal{X}$

A **line** is parametrized by 2 parameters: an angle $\theta \in \left(-\frac{\pi}{2}, -\frac{\pi}{2}\right]$ relative to the vertical axis and an offset $\eta \in \mathbb{R}$ along the horizontal axis; that is by a 2D point $\boldsymbol{x} = (\eta, \theta) \in \mathcal{X}$ (Fig. 1b).

A superposition of K line **atoms** with different amplitudes $\boldsymbol{\alpha} = (\alpha_k)_{k=1}^{K}$ can be modeled as the evalutation of a **kernel** φ over a **measure** $m_{\boldsymbol{\alpha},\mathbf{x}} = \sum_{k=1}^{K} \alpha_k \delta_{\boldsymbol{x}_k} \in \mathcal{M}(\mathcal{X})$, designated by

$$\Phi m_{\boldsymbol{\alpha},\mathbf{x}} = \int_{\mathcal{X}} \varphi(\boldsymbol{x}) \mathrm{d}m_{\boldsymbol{\alpha},\mathbf{x}} = \sum_{k=1}^{K} \alpha_k \varphi(\boldsymbol{x}_k)$$

Objectives

- Characterize the kernel $\varphi : \mathcal{X} \to \mathcal{H}$ for a given model
- From an observation $y = \Phi m + w \in \mathcal{H}$ where w represents noise, reconstruct the measure m.

GAUSSIAN LINES KERNEL

A **perfect line distribution** $\delta_{\mathscr{L}(\eta,\theta)}$ maps a function ψ in the Schwartz class $\mathcal{S}(\mathbb{R}^2)$ to its integral along the geometric line

$$\mathscr{L}(\eta, \theta) = \{(u_1, u_2) \in \mathbb{R}^2 : (u_1 - \eta)\cos\theta + u_2 \sin\theta = 0\}$$

A **Gaussian Line (GL)** can be modeled as the convolution of a perfect line $\delta_{\mathscr{L}}$ with a Gaussian point spread function ϕ:

$$\forall \boldsymbol{x} \in \mathcal{X}, \quad \varphi_{\mathrm{GL}}(\boldsymbol{x}) = \delta_{\mathscr{L}(\boldsymbol{x})} * \phi$$

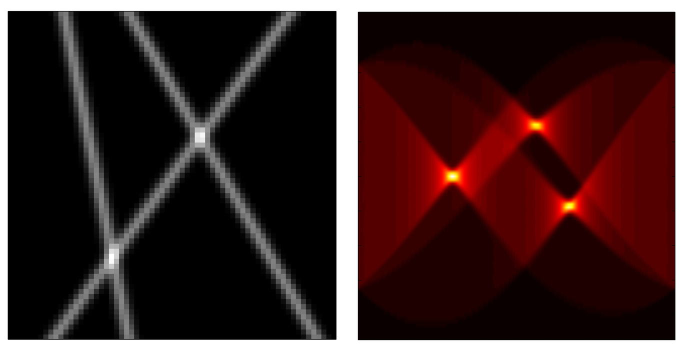

(a) (b)

FIGURE 1 – (a) Three Gaussian Lines with parameters of Experiment 1 in the noiseless case. (b) Its Radon transform in the plane (θ, η).

SPECTROGRAM CHIRP LINES KERNEL

A **linear chirp** $f_{\eta,\beta}(t) = \mathrm{e}^{2i\pi\left(\eta t + \frac{\beta}{2}t^2\right)}$ is a frequency-modulated signal with linear *instantaneous frequency* $\phi'(t) = \beta t + \eta$, represented as a line in the time-frequency plane (t, ω).

Computed with a Gaussian window, its spectrogram has an exact formulation [2] leading to the **Chirp Lines (CL)** kernel:

$$\varphi_{\mathrm{CL}}(\eta, \theta) := (t, \omega) \mapsto \sigma_{\theta,N}\, \mathrm{e}^{-\frac{2\pi\sigma^2(\omega - (N-1)(\eta + \tan(\theta) t))^2}{1 + \sigma^4 (N-1)^2 \tan^2\theta}}$$

REFERENCES

[1] Q. Denoyelle and V. Duval and G. Peyré and E. Soubies (2018). The Sliding Frank-Wolfe Algorithm and its Application to Super-Resolution Microscopy. *Inverse Problems* 36(1), 014001.

[2] S. Meignen, N. Laurent, and T. Oberlin (2022). One or two ridges ? an exact mode separation condition for the gabor transform. *IEEE Signal Processing Letters* 29:2507-2511.

[3] K. Polisano, L. Condat, M. Clausel, V. Perrier (2019) A Convex Approach to Superresolution and Regularization of Lines in Images. SIAM Journal on Imaging Sciences 12:211–258.

SLIDING FRANK–WOLFE (SFW) FOR BLASSO

BLASSO

- $f : (m, t) \in \mathcal{M}(\mathcal{X}) \times \mathbb{R} \mapsto \|y - \Phi m\|_{\mathcal{H}}^2 + \lambda t$
- $\mathrm{d}f(m,t) : (m', t') \mapsto \int_{\mathcal{X}} \Phi^*(\Phi m - y)\, \mathrm{d}m' + \lambda t'$
- $C = \{(m, t) : |m|(\mathcal{X}) \leq t \leq \frac{\|y\|^2}{2\lambda} = r\}$ a convex.

The linear form $s \mapsto \mathrm{d}f(m,t)[s]$ reaches its minimum at one extreme point of C *i.e* $s = (0,0)$ or $s = r \cdot (\pm\delta_{\boldsymbol{x}}, 1)$ for $\boldsymbol{x} \in \mathcal{X}$. For $m^j := m_{\boldsymbol{\alpha}^j,\mathbf{x}^j} = \sum_{k=1}^{j} \alpha_k^j \delta_{\boldsymbol{x}_k^j}$:

- Step 2. in Algorithm 1 $\Leftrightarrow$ $\boldsymbol{x}_*^j \in \arg\max_{\boldsymbol{x}\in\mathcal{X}} |\eta^j(\boldsymbol{x})|$
  $\lambda\eta^j(\boldsymbol{x}) = (\Phi^*(y - \Phi m^j))(\boldsymbol{x}) = \langle\varphi(\boldsymbol{x}), y - \Phi m^j\rangle_{\mathcal{H}}$
- [1] uniformly sampled $\mathcal{X}$ on a grid to find the max. We replaced this **greedy search** by finding the local max in the Radon space (see Fig. 1b).
- In step 7. m^{j+1} can be replaced by any point $\hat{m} \in C$ satisfying $f(\hat{m}) \leq f(m^{j+1})$. SFW adds a non-convex minimization step updating both the positions and the amplitudes of the spikes:
  - $\tilde{\mathbf{x}}^j = (\boldsymbol{x}_1^j, \ldots, \boldsymbol{x}_j^j, \boldsymbol{x}_*^j)$ (initial point)
  - $\tilde{\boldsymbol{\alpha}}^j = \arg\max_{\boldsymbol{\alpha}\in\mathbb{R}^{j+1}} \|y - \Phi m_{\boldsymbol{\alpha},\tilde{\mathbf{x}}^j}\| + \lambda\|\boldsymbol{\alpha}\|_1$
  - $\boldsymbol{\alpha}^{j+1}, \mathbf{x}^{j+1} = \arg\max_{\boldsymbol{\alpha},\tilde{\mathbf{x}}} \|y - \Phi m_{\boldsymbol{\alpha},\tilde{\mathbf{x}}}\| + \lambda\|\boldsymbol{\alpha}\|_1$

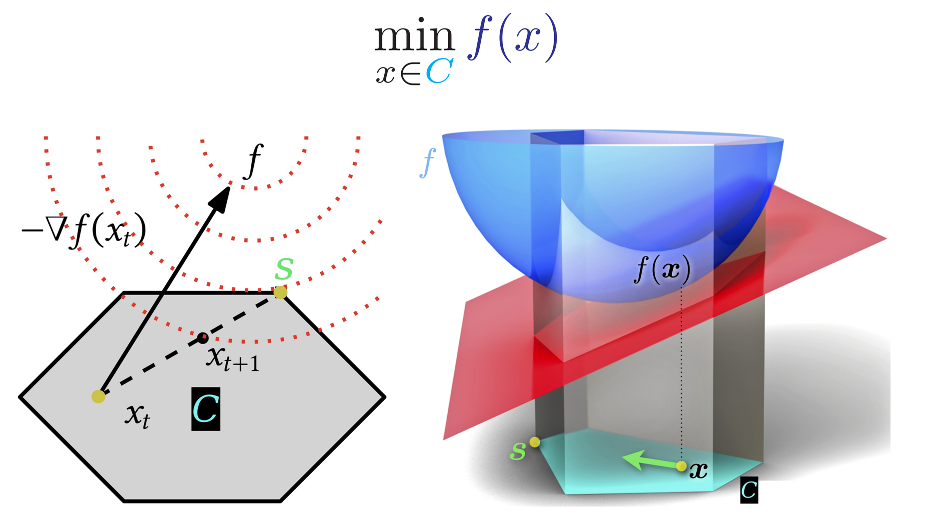

(a) FW iterations **(b)** FW in 3D

Algorithm 1 Frank–Wolfe Algorithm (FW)

1: **for** $j = 1$ **to** $K_{\max}$ **do**
2: $\quad s^j \in \arg\min_{s\in C} f(m^j) + \mathrm{d}f(m^j)(s - m^j)$
3: $\quad$ **if** $\mathrm{d}f(m^j)(s^j - m^j) = 0$ **then**
4: $\quad\quad m^\star \leftarrow m^j$ is optimal.
5: $\quad$ **else**
6: $\quad\quad \gamma^j \leftarrow \arg\min_{\gamma\in[0,1]} f(m^j + \gamma(s^j - m^j))$
7: $\quad\quad m^{j+1} \leftarrow m^j + \gamma^j(s^j - m^j)$
8: $\quad$ **end if**
9: **end for**

NUMERICAL RESULTS

Gaussian Lines. Images have a dimension of $N = 65$ and contained blurred lines corrupted by additional white noise $\boldsymbol{w} \sim \mathcal{N}(0, \sigma^2)$. We replicated three experiments from [3].

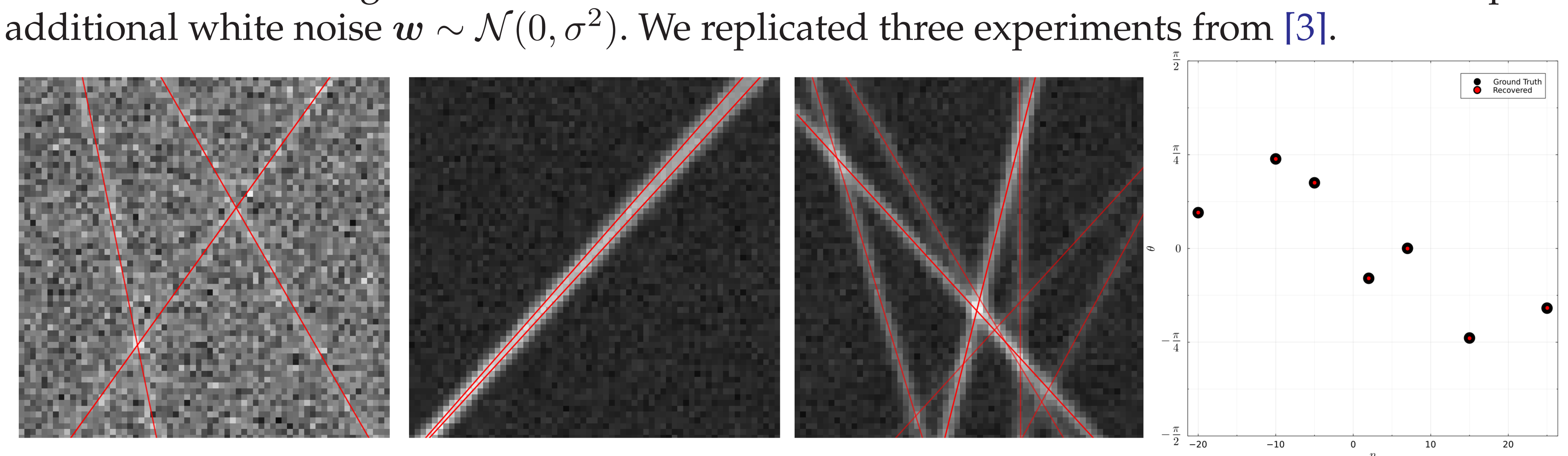

(a) (b) (c) (d)

FIGURE 3 – (a) Exp. 1 (very noisy lines), (b) Exp. 2 (very close lines plus noise), (c) Exp. 3 (more lines with different amplitudes plus noise). The estimated lines are depicted in red. (d) Estimated parameters (θ_k, η_k).

Chirp Lines. Image dimension is $N = 256$. A white noise $\boldsymbol{w} \sim \mathcal{N}(0, \sigma^2)$ is added to the 1D signal formed by the superposition of $K = 2$ chirps with equal amplitudes. The Short-Time Fourier Transform leads to a spectrogram with **interference** and noise following a χ_2 distribution.

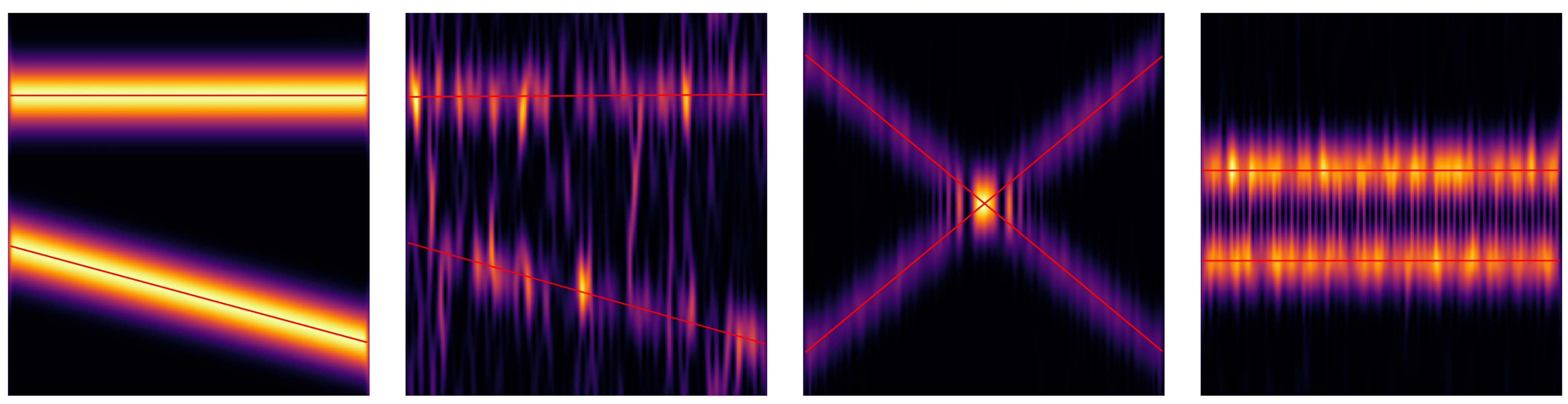

(a) (b) (c) (d)

FIGURE 4 – (a) Exp. 4 in the noiseless case, (b) Exp. 4 with no interference and high amount of noise (χ_2 distributed), (c) Exp. 5 for crossing lines with interference and moderate noise, (d) Exp. 6 for parallel close lined with more interference and moderate noise. The estimated lines are depicted in red.

	Error	Exp. 1	Exp. 2	Exp. 3	Exp. 4	Exp. 5	Exp. 6
[3]	$\overline{\Delta_\theta}$	$2 \cdot 10^{-2}$	$4 \cdot 10^{-3}$	$6 \cdot 10^{-3}$			
	$\overline{\Delta_\eta}$	$4 \cdot 10^{-2}$	$6 \cdot 10^{-1}$	$2 \cdot 10^{-1}$			
	$\overline{\Delta_\alpha}$	$1 \cdot 10^{-1}$	$4 \cdot 10^{-2}$	$2 \cdot 10^{-2}$			
Proposed approach	$\overline{\Delta_\theta}$	$\mathbf{1 \cdot 10^{-3}}$	$\mathbf{5 \cdot 10^{-4}}$	$\mathbf{2 \cdot 10^{-4}}$	$6 \cdot 10^{-3}$	$2 \cdot 10^{-3}$	$6 \cdot 10^{-4}$
	$\overline{\Delta_\eta}$	$\mathbf{2 \cdot 10^{-2}}$	$\mathbf{3 \cdot 10^{-2}}$	$\mathbf{2 \cdot 10^{-2}}$	$4 \cdot 10^{-3}$	$6 \cdot 10^{-4}$	$5 \cdot 10^{-4}$
	$\overline{\Delta_\alpha}$	$\mathbf{3 \cdot 10^{-2}}$	$\mathbf{8 \cdot 10^{-3}}$	$\mathbf{1 \cdot 10^{-2}}$	$2 \cdot 10^{-1}$	$4 \cdot 10^{-2}$	$1 \cdot 10^{-2}$

TABLE 1 – Errors on estimated parameters

CONCLUSION

- We enhanced the 2D line super-resolution technique initiated in [3].
- We proposed a new kernel characterizing ridges of linear chirps in the spectrogram.
- **Perspective**: reconstruct the ridges of more complex signals by local approximation.